

Scheduler dependent modeling of inter-cell interference in UMTS EUL

D. C. Dimitrova
and G. Heijenk

University of Twente, The Netherlands
E-mail: {d.c.dimitrova,geert.heijenk}@ewi.utwente.nl

J. L. van den Berg
University of Twente,
TNO ICT, The Netherlands

E-mail: J.L.vandenBerg@ewi.utwente.nl

Abstract—In this paper we analyze the performance of the UMTS Enhanced Uplink (EUL) in a network scenario, under various packet scheduling schemes. Besides the impact of the intrinsic differences of the scheduling schemes on EUL performance (which we studied in a previous paper for a single cell scenario), we are particularly interested in how the different scheduling schemes influence EUL performance through their impact on the characteristics of the inter-cell interference. For our analysis we use a hybrid analytical/simulation approach, originally developed for the single cell situation, and extend it to our multi cell scenario. We show that the mutual influence between neighbouring cells due to inter-cell interference is largely determined by only one or two power iteration steps, which considerably speeds up computations. Our approach takes into account both the packet-level characteristics and the flow-level dynamics due to the random user behaviour. For the considered schedulers we evaluate and compare performance measures such as the mean flow transfer time and throughput.

I. INTRODUCTION

UMTS (Universal Mobile Telecommunication System) is currently deployed in many countries around the world. The technology continued evolving towards improved spectrum utilization, with the EUL (Enhanced Uplink) technology being the latest extension on the uplink, from mobile to base station. EUL has been specified in 3GPP Release 6 of the UMTS standard [1]. The key radio resource in EUL is the maximum received power at the base station, which is shared among the active EUL users. Channel access is coordinated by the base station allocating time frames of fixed length (2 or 10 ms, termed TTI: Transmission Time Interval) to the users.

EUL-enabled devices often operate on batteries and as such have limited power capacity. Depending on its distance to the base station a device can or cannot use the total available resource on its own. In the former case throughput is optimized by single transmissions during a time slot (TTI) [2] while in the latter simultaneous transmissions by different users are a better choice [3]. A well chosen scheduling scheme which efficiently assigns the TTIs to EUL users can enable flexible resource allocation and optimize service. In order to select among different schemes, we need an appropriate evaluation approach and a realistic evaluation scenario.

In the literature two main approaches towards EUL scheduling evaluation are most common. One the one side, dynamic system simulation is used, see e.g. [4], incorporating many details of the system traffic behaviour,

but usually being very time-consuming. On the other side, analytical studies provide fast evaluation but often simplify system specifics. For example, [5] considers the behaviour of the scheduler but not dynamically changing flow traffic. We have developed a hybrid analysis exploiting the advantages of both approaches. Our approach combines mathematical analysis, which includes packet level parameters, and simulation, capturing the system behaviour at flow level. It allows us to evaluate the impact of both environment, i.e. inter-cell interference, and scheduling scheme as well as their mutual influence. This unique combination enables evaluation of a diversity of system scenarios and supports fast evaluation.

Not many studies consider both environment and scheduler specifics at the same time as our work does. Interesting studies, which incorporate flow level traffic behaviour and discuss scenarios similar to ours, are [6],[7] and [8]. In particular, [8] analyzes the flow level performance of two schedulers in a single cell. However, it does not differentiate in users' power capacity thus diminishing the impact of the user's location. In a later study [9], the same authors consider the impact of inter-cell interference but without capturing the impact of the particular scheduling scheme used in the network.

In the present paper we consider a network scenario with a central reference cell (RC) and six neighbour cells (NCs). Three basic scheduling schemes of the Round Robin family are compared in performance. The schemes are described in Section II and their performance is evaluated in Section IV.

The main contribution of our study lays in the modeling of inter-cell interference as a process which in fact depends on the applied scheduling scheme. Several aspects of this are discussed. First, we show how the particular scheduler determines the inter-cell interference process. Since the modeling of this process is crucial for correct system representation, we provide several possible modeling approaches which take into account the scheduling scheme. Second, we consider the mutual influence that neighbouring cells have on each other in terms of inter-cell interference. In particular, we are interested in the resulting iterative process of power adaptation in each cell. We show that the mutual influence can be largely captured by only one or two iterations, which considerably speeds up performance evaluation. Finally, as an extension of our previous work with a single NC from [10], for the different schedulers, the performance at the RC is compared in

the presence of inter-cell interference from the six NCs. Performance measures such as mean flow transfer time and coverage are used.

The rest of the paper is organized as follows. Section II introduces the three different scheduling schemes. In Section III we describe the network scenario and present the analytical approach taken in this paper. The numerical results are discussed in Section IV. Finally, Section V concludes our work.

II. SCHEDULING SCHEMES FOR ENHANCED UPLINK

We consider three scheduling schemes, denoted *one-by-one* (OBO), *partial parallel* (PP) and *full parallel* (FP); see Figure 1. All three belong to the class of channel-oblivious schedulers, i.e. channel access is granted irrespective of channel conditions. The schemes differ in their preference for granting consecutive or parallel channel access and in their capability to fully utilize the available channel resource. This resource is the maximum received power at the base station which we term *total available budget* B . The received powers can originate from users inside and outside the cell. All powers from other than EUL users in the own cell we refer to as interference. The channel resource available to EUL users, after the interference is subtracted from B , is termed *EUL budget* B' . The main task of the packet scheduler is to distribute the EUL budget B' among all active EUL users in the cell. We want to identify the scheduling scheme maximizing the throughput at flow level.

The budget distribution is scheduler specific and is illustrated in Figure 1. In each TTI, the *OBO* scheduler assigns the full EUL budget B' to a single user, serving all users in a Round Robin order [8]. The total time, i.e. number of TTIs, necessary to serve all active users once is denoted as *transmission cycle*. Thus, for OBO, the transmission cycle equals the number of active EUL users. The received power of a user depends on its maximum attainable power P_{max}^{rx} and its distance to the base station and cannot exceed the available EUL budget B' , i.e. $P^{rx} = \min(P_{max}^{rx}, B')$. Such single user policy has the benefit of no intra-cell interference from other EUL users [2]. At the same time it also appears to be inefficient when a user is incapable to utilize the granted resource B' in full. The latter phenomenon manifests at long distances and is a consequence of the combination limited battery capacity and path loss.

The *FP* scheduler [8] has as primary objective the total resource utilization. It aims to do so by serving all active users simultaneously, resulting in transmission cycle of 1 TTI, and granting each user a fraction of the EUL budget. The fraction size depends on the number of active users and on their maximum attainable powers. Hence we can write:

$$P^{rx} = \frac{P_{max}^{rx}}{P_{total}} B',$$

where P_{total} denotes the total power budget requested by all active users. The full resource utilization comes on the

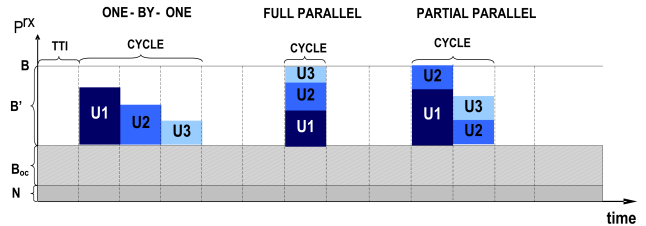


Figure 1. Illustration of the packet handling of the considered EUL scheduling schemes.

cost of reduced received powers and increased intra-cell interference compared to a single user policy, i.e. OBO.

The hybrid *PP* scheduler aims to combine the advantages of the other two schemes. The active users are assigned the maximum attainable received power, i.e. $P^{rx} = \min(P_{max}^{rx}, B')$, and, when EUL budget is available, scheduled simultaneously in the same TTI. Any unserved users are left for subsequent TTI(s). This scheduling strategy results in high received powers and yet shorter transmission cycle than the OBO scheme. It is our expectation that due to its specifics the PP scheme should perform best.

As shown in [10], the particular ordering of the active users within the cycle does not significantly influence the performance of the schedulers.

III. MODELING AND ANALYSIS

In order to evaluate the three schedulers in a realistic network we consider a model of a seven-cell scenario. The network scenario and the modeling assumptions are presented in Section III-A and Section III-B respectively. The application of the combined analysis to the seven-cell scenario is presented in Section III-C.

A. System model

The network scenario considers a central reference cell (RC), where the schedulers' performance is evaluated, and six neighbour cells (NCs), see Figure 2. A second tier of cells is not necessary since we concentrate on the reference cell. The distance between the base stations of two near cells is taken to be double the cell radius. The available budget in the RC depends on the inter-cell interference caused by the NCs. However, the behaviour of a NC is considered to be autonomous of the behaviour of the RC, for more detail see Section III-C3.

To differentiate in users' position, the cells are split up into K concentric zones with the same area, i.e. $i = 1, \dots, K$. Zone i is characterized by a distance d_i to the base station, which is measured from the outside border of the zone, and a corresponding path loss denoted by $L(d_i)$. In addition, in order to enable precise characterization of the inter-cell interference, each neighbour cell is split up in S equally sized sectors, i.e. $j = 1, \dots, S$. The intersection of zones and sectors in the NC determines segments characterized by a distance d_{ij} and corresponding path loss $L(d_{ij})$ to the base station of the reference cell.

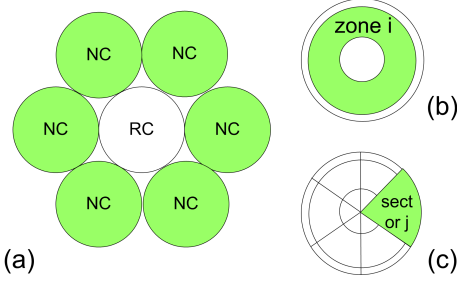


Figure 2. Modeling approach: (a) seven cell scenario with a central reference cell and six neighbour cells; (b) division of the reference cell in zones; (c) division of a neighbour cell in zones and sectors.

At a given time, the RC state $\underline{n} \equiv (n_1, n_1, \dots, n_K)$ describes the number of active EUL flows n_i in zone i . For a NC each element n_i is a vector of the form $\equiv (n_{i1}, n_{i2}, \dots, n_{iS})$ which represents the number of active flows for all segments j , within each zone i .

B. Assumptions

As illustrated in Figure 1, the received interference power at the base station originates from several sources: (i) constant thermal noise level N ; (ii) inter-cell interference I_{oc} ; (iii) interference I_{EUL} from simultaneously active EUL users in the cell; and (iv) self-interference represented by parameter ω , which is due to the effects of multipath fading. As we will show later inter-cell interference is a time variable process. A dynamic, scheduler-specific reservation B_{oc} is introduced in the model to cope with anticipated inter-cell interference, see Section III-C2. What is left of B after we subtract thermal noise N and inter-cell interference B_{oc} is the resource available for serving the EUL flows within the cell, i.e. EUL budget B' .

A number of additional assumptions are made at the *user* level. Users located in the same zone have the same distance to the base station. EUL flows are generated according to a spatially uniform Poisson arrival process with rate λ . Therefore, given equal area size, the EUL flow arrival rate per zone λ_i is equal to λ/K , $i = 1, \dots, K$. For a segment (i, j) of a NC the arrival rate is then $\lambda_{i,j} = \lambda/KS$. The flow size is exponentially distributed with mean F (in kbits). All users have the same maximum transmit power P_{max}^{tx} but different maximum received power at the base station $P_{i,max}^{rx}$ due to the zone-dependent path loss. No user mobility is considered.

C. Mathematical analysis

The analysis, for each of the scheduling schemes described in Section 2, is an extension of our work in [10]. First, in Subsection III-C2 the inter-cell interference process from a neighbour cell is presented followed by a discussion on its modeling in the reference cell. Next, in Subsection III-C3 the mutual impact near cells have of each others performance is examined. The analysis of both RC and NC is based on a flow level modeling and analysis approach for a single cell scenario presented in a previous paper, see [11]. We will first briefly summarize

this approach and next we will move on to present the modeling of the inter-cell interference.

1) *Basic Analysis of a Single Cell*: Consider a single cell scenario. The system state \underline{n} fully describes the users' population. The data rate $r_i(\underline{n})$ of a user in zone i , at the time it receives service we term *instantaneous rate* and is given by,

$$r_i(\underline{n}) = \frac{r_{chip}}{E_b/N_0} \cdot \frac{P_i^{rx}}{I_{EUL}(\underline{n}) - \omega P_i^{rx} + B_{oc} + N}, \quad (1)$$

where r_{chip} is the system chip rate and E_b/N_0 is the energy-per-bit to noise ratio. A self-interference of 10% of the own signal is assumed, i.e. $\omega=0.9$. The interference from EUL users $I_{EUL}(\underline{n})$, for the different scheduling schemes, is given by

$$I_{EUL}(\underline{n}) = \begin{cases} P_i^{rx} & \text{for OBO} \\ \min\{\sum_{i=1}^K n_i P_i^{rx}, B'\} & \text{for PP and FP} \end{cases}$$

In OBO a scheduled users does not experience interference from other EUL users. In FP all other active EUL users interfere and in PP only the one scheduled in the same TTI. The choice of B_{oc} depends on the modeled cell - a constant for the NCs and a time variable for the RC and is discussed in Section III-C2.

The actual effective throughput of EUL users depends on the transmission cycle and is lower or equal the instantaneous rate. This so-called *state-dependent throughput* $R_i(\underline{n})$ is given by

$$R_i(\underline{n}) = \frac{r_i(\underline{n})}{c(\underline{n})} \quad (2)$$

The scheduling cycle length in state \underline{n} is determined by the applied scheduling scheme as follows:

$$c(\underline{n}) = \begin{cases} \sum_{i=1}^K n_i & \text{for OBO} \\ \frac{\sum_{i=1}^K n_i P_{i,max}^{rx}}{B'} & \text{for PP} \\ 1 & \text{for FP} \end{cases} \quad (3)$$

For each of the schedulers, the system's behaviour at flow level can be described by a K -dimensional continuous time Markov chain with transition rates λ_i (representing that new users may become active in zone i) and $n_i \times R_i(\underline{n})/F$ (representing that active user in zone i may 'depart', i.e. complete its flow transfer), $i = 1, \dots, K$. Note that the packet level details are captured in the analytically calculated transition rates. The steady-state distribution of the Markov chain can be derived by standard techniques, e.g. numerical solution of the balance equations or simulation. Since $R_i(\underline{n})$ is state dependent parameter numerical solutions, when feasible, are cumbersome. Given, Markov models are very attractive to simulate due to fast computation we have chosen simulation. From the steady-state distribution of the Markov chain performance measures such as the zone-specific mean flow transfer time can be determined, see [11].

Table I
IMPACT OF FIRST ITERATION ON RECEIVED POWER LEVELS

$I_{oc,av} * 10^{-14}$	Watt	1	2	3	4
Partial parallel					
max δP	%	6%	12%	22%	40%
$Pr(\delta P > 5\%)$	%	0.00%	0.01%	0.04%	2.00%
Full parallel					
max δP	%	10%	21%	39%	73%
$Pr(\delta P > 5\%)$	%	0.02%	0.13%	0.19%	45%

$I_{oc,av}$ - mean inter-cell interference; max δP - maximum power change; $Pr(\delta P > 5\%)$ - probability the power change to be bigger than 5%.

2) *Inter-cell Interference Modeling at the RC:* Given a state \underline{n} in the NC and knowing the path loss matrix $L(d_{ij})$ to the base station of the RC, the I_{oc} generated in each TTI of the transmission cycle for the duration of that state is fully determined. For the FP scheme the transmission cycle length equals one, and hence the inter-cell interference in a given system state is just a single value. For the OBO and PP schemes, the inter-cell interference varies when the cycle length is bigger than one TTI. Thus, for OBO and PP, I_{oc} changes not only at flow level but also at TTI level. A real system can adapt to the changes at flow level but 2 ms is too short period to react to the changes at the TTI level. In our model we address the flow level changes by dynamically adapting the reservation B_{oc} to the sum of the interference levels from the NCs. Whenever the state in any of the NCs changes so does the inter-cell interference generated by that cell and B_{oc} should be adapted.

To cope with the TTI level changes a single value is selected to represent the TTI variation of I_{oc} within a transmission cycle. We have adopted two approaches to select a representative value - selecting the average of all I_{oc} values generated over the transmission cycle or the maximum realized value. This representative value is taken for the computation of the reservation level B_{oc} during the given state. Taking an average value brings the risk that the real interference is rather often higher than the reservation B_{oc} . Using the maximum value avoids the problem but it also implies that there will be over-reservation. This is especially true for users located at the edge of the NC close to the RC which generally have long service times and generate high inter-cell interference. Despite the shortcomings of both approaches they allow us to evaluate the system for two extremes concerning the realized I_{oc} , leading to upper and lower boundary of the performance.

The single cell analysis from Section III-C1 when applied to the RC, with K zones, and a NC, with $K \times S$ segments, results in a K - and $K \times S$ -dimensional Markov model respectively. Hence the whole seven cell network can be described by a $(K + K \times S)$ -dimensional M/G/1 Markov model with several service classes. Trying to find its steady-state distribution by numerical methods is rather challenging as well as very time consuming. Therefore we have chosen to simulate the actual state transitions in order to derive performance measures such as mean flow transfer time.

3) *Mutual interaction RC - NC:* In a real network the RC and NC influence each other in terms of inter-cell interference and thus available budget. This mutual influence can be modeled by an iterative process which gradually leads to equilibrium powers. Ideally, these powers should be used to determine instantaneous rates. However, big number of iterations could lead to an unacceptable long computation time. Therefore, we have evaluated the potential improvements iterations could bring to our modeling and how important it is to account for them.

Table I summarizes the results of four independent experiments. The experiments differ in the average inter-cell interference $I_{oc,av}$ generated by the NCs. Five of the NCs generate constant inter-cell interference while in the sixth NC and the RC the number of active EUL users dynamically changes. For each of 600 000 simulated states, i.e. after each state change, we have applied the iterative power process. Eventually, we were able to determine the probability $Pr(\delta P > x)$ that the power change at the second iteration step exceeds a certain threshold x ; and the maximum recorded power change $\max \delta P$ taken over all state changes. As Table I shows $\max \delta P$ is considerable in all experiments for both PP and FP. However, these large changes seem to occur for specific, rare state changes; thus the overall probability of a power change to be bigger than 5% is negligible. Given power changes decrease in the iteration number, based on the results we consider it sufficient to account only for the first iteration, i.e. the influence of the NCs on the RC.

IV. NUMERICAL RESULTS

The performance of the three scheduling schemes is evaluated at flow level in the presence of inter-cell interference. We developed a generic simulator in Matlab which derives the steady-state distribution of our model based on a large number of flow level events, i.e. 100 000 flow initiations or departures per cell. The choice to use Markov chains to model flow level behaviour paid off in relatively short running times. For example, our simulations with confidence intervals of about 1% took typically about 20 – 30 minutes when run on a Intel Core 2 processor at 1.83 GHz with 2GB RAM.

As performance measures we have chosen mean flow transfer times and coverage. With coverage we denote the maximum distance at which a particular data rate is deliverable. Coverage is evaluated idealistically, denoted C_{id} , based on instantaneous data rates and without considering inter-cell interference; and realistically, denoted C_r , based on flow dynamics and present inter-cell interference.

A. Parameter Settings

In the numerical experiments we apply a system chip rate r_{chip} of 3840 kchips/s, a thermal noise level N of -105.66 dBm and a noise rise target η , derived from an operator-specified noise rise target, of 6 dB. Hence the total received power budget can be derived $B = \eta \cdot N$. A self-interference of 10% is considered, i.e. $\omega = 0.9$. The assumed path loss is given by $L(d) = 123.2 + 35.2 \log_{10}(d)$ (in dB) with d the distance in kilometers.

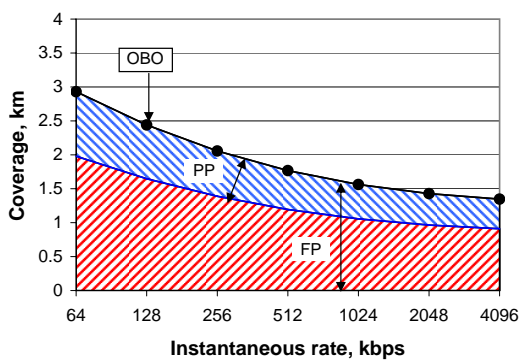


Figure 3. Idealistic system coverage C_{id} based on instantaneous rates, for OBO, PP and FP scheduler

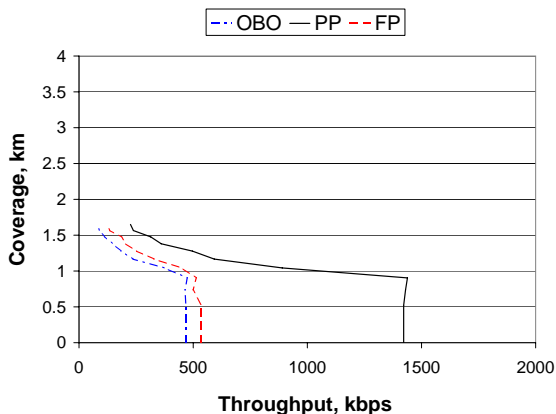


Figure 4. Realistic system coverage C_r accounting for flow level dynamics and inter-cell interference for OBO, PP and FP scheduler; cell arrival rate of 0.6 flows/sec

All users have $P_{\max}^{tx} = 0.125$ Watt; and each EUL flow is characterized by a an E_b/N_0 target of 5 dB and mean file size of $F = 1000$ kbit. In the experiments we let the call arrival rate vary. Both types of cells have a cell radius of 1.65 km and are split in $K = 10$ zones¹ and the neighbour cells in $S = 6$ sectors (see Figure 2).

B. System Coverage

We begin with a discussion on the idealistic coverage C_{id} . Although C_{id} disregards flow behaviour and inter-cell interference, it allows us to isolate the impact of the scheduling scheme on the coverage. The corresponding graphs are presented in Figure 3 and require careful analysis incorporating knowledge of the schedulers.

A one-by-one scheduler has an instantaneous rate which is not influenced by interference from other EUL users. Therefore, from Equation (1) a straightforward relation between rate and coverage can be established and represented by a single line graph. On the contrary, a scheduler that allows parallel transmissions inherently suffers from

¹Extensive numerical experiments showed that this granularity is sufficient for our purposes.

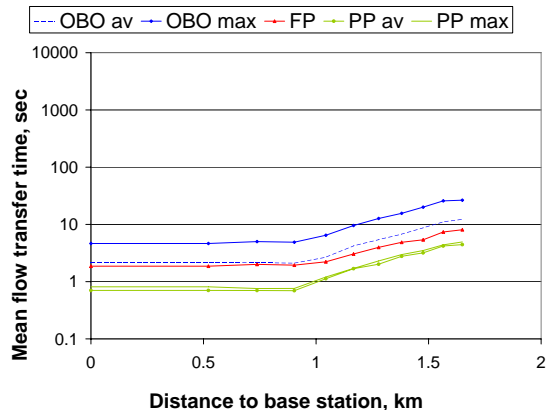


Figure 5. Mean flow transfer time for a load of 0.6 flows/sec per each zone in the RC

interference from other EUL users. Hence coverage is interference dependent and can be represented by an area of possible realizations. Note that PP and FP with one user in the cell behave as a OBO scheme which sets their maximum realized coverage. With parallel transmissions the worst case interference is when the EUL budget is full. Since PP preserves the maximum transmission powers, we can determine minimum coverage and thus PP has a two-side limited coverage area, see Figure 3. Such positive minimum does not exist for full parallel because by definition the scheme does not set a limit to power decrease. This explains why its coverage area hypothetically can drop down to zero, see Figure 3.

Working with C_{id} is straightforward but does not account for the time aspect of scheduling, i.e. the transmission cycle. Therefore we calculate a realistic coverage C_r which takes into account the effect of the flow level dynamics and the inter-cell interference. Figure 4 shows that the realized throughput, for a given network load, are lower than the ones from Figure 3. This is explained by the negative impact of inter-cell interference and transmission cycle on the effective throughput. More interesting is the difference in coverage between the schedulers. OBO shows to have the worst coverage even if it had the best in Figure 4. The advantages of a single user policy in terms of low intra-cell interference cannot compensate for the poor efficiency on a larger time scale, i.e. long transmission cycle. PP outperforms the other two schemes because of optimal combination of parallel transmissions at maximum transmit power.

C. Mean Flow Transfer Time

The mean flow transfer time is an indicator of the service a mobile receives for the duration of its file transfer. As Figure 5 shows the mean flow transfer time inherits the dependency of path loss from the distance. Long transmission path, i.e. for far located user, means high path loss and low received power. During the evaluation of the OBO and PP schemes we have used both the average and maximum reservation B_{oc} to model inter-cell interference at the RC. Therefore OBO and PP are represented in

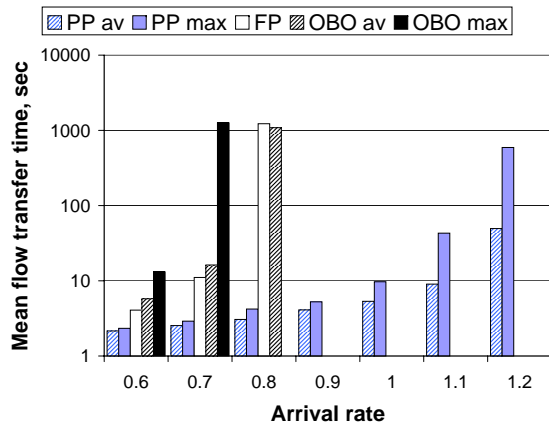


Figure 6. Mean flow transfer time aggregated for all zones and for a range of arrival rates.

Figures 5 and 6 by two graphs each. It seems that PP can effectively combine the advantages of the other two schemes and by this it outperforms them. On the one hand, FP, although fast to reassign the budget, suffers from decreased received powers and increased intra-cell interference. On the other hand, the performance of OBO, which keeps the maximum received powers, suffers from the long cycle, consequence of the single-user policy.

Figure 6 shows the same results but spanned over a range of arrival rates. An advantage of working with range of arrival rates is that we can identify tendencies. For example, the impact of the B_{oc} reservation strategy, i.e. average or maximum. The difference between the two strategies depends on the cycle length. Longer cycle decreases the contribution of the maximum value on the average and thus causes significant differences between the maximum and average reservation and thus in the registered mean flow transfer times. This explains why the results for OBO, which has long cycle, lay far from each other and the ones for PP are close in value. We can conclude that for a PP scheme it is irrelevant which B_{oc} reservation is chosen. However, if OBO is applied a better approach towards reservation is to use for example the 90% quantile of the inter-cell interference distribution.

Big values for the mean flow transfer time indicates that the system reaches its stability limit. For example, a OBO scheme with maximum reservation reaches instability around an arrival rate of 0.7 flows/sec. It appears that a system with partial parallel scheduler has twice as big capacity as a system with OBO or FP scheme. The less efficient the scheduler and the longer the service time the faster instability is reached. This explains why in Figure 6 OBO with maximum reservation reaches saturation first while a PP scheduler with average reservation - last. An expectation which is confirmed by the results in Figure 6.

V. CONCLUSIONS

We analyzed a UMTS/EUL network scenario with a central reference cell RC and six neighbour cells NCs. Our goal was to observe the influence of inter-cell interference on flow level performance, for different scheduling

schemes. The schemes differ in the strategy used to assigne channel access to the users and thus deliver different base station resource utilization.

Using a hybrid analytical/simulation approach we were able to evaluate performance parameters such as mean flow transfer time and coverage. The results are consistent with our previous studies on single cell scenario [11], [10] and show that a PP schemes is the best in performance followed by FP and OBO. Furthermore, we show that the inter-cell interference is a scheduler specific dynamic process and requires appropriate modeling. Particularly interesting contribution are the results indicating that the mutual influence neighbour cells have on each other's performance can be largely captured by a single iteration speeding considerably computations.

More advanced studies on EUL packet scheduling are surely possible. An especially attractive direction for further research is investigating the effect of mobility.

REFERENCES

- [1] G. T. 25.309, "FDD Enhanced Uplink; Overall Description."
- [2] S. Ramakrishna and J. M. Holtzman, "A scheme for throughput maximization in a dual-class CDMA system." ICUPC '97, San Diego, USA, 1997.
- [3] H. Holma and A. Toskala, *HSDPA/HSUPA for UMTS*. John Wiley & Sons Ltd, 2006.
- [4] C. Li and S. Papavassiliou, "On the fairness and throughput trade-off of multi-user uplink scheduling in WCDMA systems," in *IEEE VTC '05 (Fall)*, Dallas, USA, 2005.
- [5] K. Kumaran and L. Qian, "Uplink scheduling in CDMA packet-data systems," in *Wireless Networks*, vol. 12, 2006, pp. 33–43.
- [6] G. Fodor and M. Telek, "Performance analysis of the uplink of a CDMA cell supporting elastic services," in *Networking 2005, Waterloo, Canada*, 2005.
- [7] J. Voigt and K. Pannhorst, "Optimizations on scheduling strategies for enhanced uplink on WCDMA," in *VTC Spring, 2007*, pp. 1172–1176.
- [8] A. Mäder and D. Staehle, "An analytical model for best-effort traffic over the UMTS enhanced uplink," in *IEEE VTC '06 (Fall)*, Montreal, Canada, 2006.
- [9] T. Liu, A. Mäder, D. Staehle, and D. Everitt, "Analytic modeling of the UMTS enhanced uplink in multi-cell environments with volume-based best-effort traffic," in *IEEE ISCIT '07*, Sydney, Australia, 2007.
- [10] D. Dimitrova, H. van den Berg, G. Heijenk, and R. Litjens, "Impact of inter-cell interference on flow level performance of scheduling schemes for the UMTS EUL," in *WiMob '08*, Avignon, France, 2008.
- [11] D. C. Dimitrova, H. van den Berg, G. Heijenk, and R. Litjens, "Flow-level performance comparison of packet scheduling schemes for UMTS EUL," in *WWIC '08, Tampere, Finland*, vol. 5031, 2008.